Since January 2020 Elsevier has created a COVID-19 resource centre with free information in English and Mandarin on the novel coronavirus COVID-19. The COVID-19 resource centre is hosted on Elsevier Connect, the company's public news and information website.

Magnetic Resonance Imaging 79 (2021) 13–19

Contents lists available at ScienceDirect

Magnetic Resonance Imaging

journal homepage: www.elsevier.com/locate/mri

Case Report

Chest MRI of patients with COVID-19

Yu A. Vasilev [a,1], K.A. Sergunova [a,1], A.V. Bazhin [a,1], A.G. Masri [b,1], Yu N. Vasileva [c,1], D. S. Semenov [a,1], N.D. Kudryavtsev [a,1], O. Yu Panina [a,1,*], A.N. Khoruzhaya [a,1], V.V. Zinchenko [a,1], E.S. Akhmad [a,1], A.V. Petraikin [a,1], A.V. Vladzymyrskyy [a,1], A.V. Midaev [b,1], S.P. Morozov [a,1]

[a] Research and Practical Clinical Center for Diagnostics and Telemedicine Technologies of the Moscow Healthcare Department, Moscow, Russia
[b] Imed Clinic, Grozny, Chechen Republic, Russia
[c] A.I. Evdokimov Moscow State University of Medicine and Dentistry, Moscow, Russia

ARTICLE INFO

Keywords:
COVID-19
Magnetic resonance imaging
Computed tomography
Pneumonia
Chest MRI

ABSTRACT

During the pandemic of novel coronavirus infection (COVID-19), computed tomography (CT) showed its effectiveness in diagnosis of coronavirus infection. However, ionizing radiation during CT studies causes concern for patients who require dynamic observation, as well as for examination of children and young people. For this retrospective study, we included 15 suspected for COVID-19 patients who were hospitalized in April 2020, Russia. There were 4 adults with positive polymerase chain reaction (PCR) test for COVID-19. All patients underwent magnetic resonance imaging (MRI) examinations using MR-LUND PROTOCOL: Single-shot Fast Spin Echo (SSFSE), LAVA 3D and IDEAL 3D, Echo-planar imaging (EPI) diffusion-weighted imaging (DWI) and Fast Spin Echo (FSE) T2 weighted imaging (T2WI). On T2WI changes were identified in 9 (60,0%) patients, on DWI – in 5 (33,3%) patients. In 5 (33,3%) patients lesions of the parenchyma were visualized on T2WI and DWI simultaneously. At the same time, 4 (26.7%) patients had changes in lung tissue only on T2WI. (P(McNemar) = 0,125; OR = 0,00 (95%); kappa = 0,500). In those patients who had CT scan, the changes were comparable to MRI. The results showed that in case of CT is not available, it is advisable to conduct a chest MRI for patients with suspected or confirmed COVID-19. Considering that T2WI is a fluid-sensitive sequence, if imaging for the lung infiltration is required, we can recommend the abbreviated MRI protocol consisting of T2 and T1 WI. These data may be applicable for interpreting other studies, such as thoracic spine MRI, detecting signs of viral pneumonia of asymptomatic patients. MRI can detect features of viral pneumonia.

1. Introduction

The novel coronavirus disease (COVID-19) in some cases is complicated by severe damage of the respiratory system. Recommendations on diagnostics and treatment of suspected for viral pneumonia patients require chest computed tomography (CT).

However, CT scans may not be available due to increased workload on CT rooms during a pandemic. Unfortunately, X-ray and sonography used in such cases do not allow to estimate a volume of lung lesions; therefore, alternative diagnostic methods are required.

The diagnosis of SARS-CoV-2 coronavirus infection is based on the comprehensive approach that includes epidemiological history, clinical manifestations, laboratory test results and lung imaging. The above methods are both useful and limited. PCR test has a false-negative rate of at least 30%. The use of chest CT for screening for COVID-19 is justified in patients with clinical and epidemiological suspicions, especially with negative results of SARS-CoV-2 RT-PCR test [1]. A current pandemic has highlighted the importance of CT scan in the objective diagnostics and dynamic assessment of COVID-19 pneumonia, as the more sensitive and effective method than X-ray. Besides that, performing chest CT scan contributes to early detection, severity assessment, and treatment effects monitoring with or without confirmation of SARS-CoV-2 [2,3].

The purpose of this study was to evaluate the possibility of using chest magnetic resonance imaging (MRI) as the alternative, non-ionizing

* Corresponding author at: 24, Petrovka st, Moscow 127051, Russia.
E-mail addresses: kristi.sergunova@gmail.com (K.A. Sergunova), avbazhin@yandex.ru (A.V. Bazhin), amir.masri6@gmail.com (A.G. Masri), drugya@yandex.ru (Y.N. Vasileva), d.semenov@npcmr.ru (D.S. Semenov), n.kudryavtsev@npcmr.ru (N.D. Kudryavtsev), olgayurpanina@gmail.com (O.Y. Panina), a.khoruzhaya@npcmr.ru (A.N. Khoruzhaya), v.zinchenko@npcmr.ru (V.V. Zinchenko), e.ahmad@npcmr.ru (E.S. Akhmad), alexeypetraikin@gmail.com (A.V. Petraikin), a.vladzimirsky@npcmr.ru (A.V. Vladzymyrskyy), amidaev@list.ru (A.V. Midaev), morozov@npcmr.ru (S.P. Morozov).
[1] These authors contributed equally to this work.

https://doi.org/10.1016/j.mri.2021.03.005
Received 21 July 2020; Received in revised form 9 March 2021; Accepted 9 March 2021
Available online 13 March 2021

Table 1
Baseline patients characteristics.

Subject	
Numder of patients	15
Age (years)	41 ± 13
Male/female	3/12
Flu-like symptoms (axillary hyperthermia >37.5 °C^ fatigue, weak or ineffective cough)	9 (60%)
Pneumonia Symptoms (severe cough, shortness of breath, chest pain)	2 (13%)
PCR positive	4 (26.7%)

method for patients with viral pneumonia. Applying this method, among others, for monitoring COVID-19 patients during and after therapy may increase overall effectiveness of the radiology department.

2. Materials and methods

2.1. Study design

This retrospective observational study was approved by the Ethics Committee for the Protection of Human Subjects of Morozov Children University Hospital of Moscow Healthcare Department (Approval N°. 156). This study includes a series of 15 cases performed at the Hospital of Chechen Republic, Russia in April 2020. Age of patients ranged from 26 to 69 years; the average age was 41 ± 13 years. 9 (60%) patients had cold-like symptoms. Also, 2 (13%) patients had cough, shortness of breath, and chest pain. 4 (26.7%) patients did not have any complaints. 4 (26.7%) patients had SARS-CoV-2-positive results of polymerase chain reaction (PCR) test (Table 1). All these 4 patients were medical employees of the intensive care unit at the infectious diseases department.

2.2. MRI scan

All patients underwent chest MRI scan in accordance with the concept "less scan time, more information". The study was conducted on 3 T scanner (Signa Pioneer, GE) in the supine position using the abdominal and spinal radiofrequency coils. The center of the abdominal coil was positioned at the mid-sternum. To minimize dynamic artifacts associated with respiratory movements, the RF coil was fixed. The central laser beam was positioned at the mid-sternum.

First of all, T2-weighted images (T2WI) were obtained in three planes using a Single-shot Fast Spin Echo (SSFSE) with following parameters: TR 2339.3 ms, TE 89 ms, flip angle 90°, FOV 450–450 mm, matrix 384 × 256, slice thickness 6 mm, spacing between slices 6 mm, number of averages 0.6, k-space filling method – Cartesian. Then these images were applied for planning axial Fast Spin Echo (FSE) T2WI.

T1-weighted images (T1WI) were performed by LAVA 3D and IDEAL 3D. For LAVA 3D, scan parameters were TR 4 ms, TE 2.2 ms and 1,1 ms, flip angle 10°, FOV 400–400 mm, matrix 288 × 288, slice thickness 3 mm, spacing between slices 1,5 mm, number of averages 0.7 with WATER and FAT fractions, in-phase/out-phase. For IDEAL 3D, scan parameters were TR 5,8 ms, TE 2.5 ms, flip angle 3°, FOV 440–440 mm, matrix 256 × 256, slice thickness 10 mm, spacing between slices 10 mm, number of averages 0.7 with WATER and FAT fractions, in-phase/out-phase.

Table 2
Comparison of the proportion of patients with the presence of lesions on T2 WI and DWI.

DWI/T2 WI	No	Yes	Summary
No	6 (40,0%)	4 (26,7%)	10 (66,7%)
Yes	0 (0,0%)	5 (33,3%)	5 (33,3%)
Summary	6 (40,0%)	9 (60,0%)	15 (100,0%)
P(McNemar)	0,125		
OR (95% CI)	0,00 (0,00; 1,51)		
kappa	0,500		

Diffusion-weighted imaging (DWI) was performed by EPI pulse sequence TR 10000 ms, TE 62.3 ms, flip angle 89°, FOV 400–400 mm, matrix 128 × 140, slice thickness 5 mm, spacing between slices 5 mm, number of averages 1, b-values: 50, 800 s/mm^2, no respiratory synchronization was used.

In addition, Fast Spin Echo (FSE) T2WI were obtained in axial plane with following parameters: TR 2125 ms, TE 82.7 ms, flip angle 111°, FOV 400–400 mm, matrix 448 × 256, slice thickness 5 mm, spacing between slices 5 mm, number of averages 1, R–L phase encoding. The scan was divided into parts (covers, batches) to collect data from separate blocks of slices and reduce movement artifacts.

The number of averages for SSFSE, LAVA-Flex and EPI series were chosen not more than 1 in order to reduce blur artifacts associated with non-availability of respiratory gating. The study was conducted with free breathing, without the use of a physical respiratory trigger, but only using automatic synchronization on the movement of the diaphragm in order to optimize the acquisition time.

All safety measures have been followed in accordance with the current recommendations. With the onset of the pandemic and the increase in the number of COVID-19 cases, the admission of scheduled patients in our department was suspended. During the examination of patients suspected for COVID-19, all safety measures were taken, namely: all department personnel was using personal protective equipment and FFP2 respirators. Patients were wearing a surgical mask without ferromagnetic elements while they were in the department and during the examination. In the control room, the air disinfection unit was operating in normal mode. In addition, all parts of the scanner that came into contact with patients were covered by disposable covers, which were disposed after each patient immediately. After the completion of the study, the scanner's surfaces were disinfected. Also, different doors were used for entrance and exit in order to separate patient flows.

2.3. CT scan

Three patients underwent a CT scan after MRI (in less than two days). We used a 128-slice CT scanner (Revolution EVO, GE) and a standard clinical protocol: 120 kV, with adaptive tube current modulation, exposure time 400 ms, slice thickness 1.25 mm, spaces between slices 0.5 mm, LUNG reconstruction filter. The average effective dose was 2 mSv.

2.4. Radiologic assessment

Patient studies were analyzed by 5 radiologists with more than 10 years of experience in interpreting MR-images. As a hypothesis for the diagnosis of COVID-19 pneumonia based on MRI scan, we borrowed the criteria used for the evaluation of CT images (presence of zones of ground glass opacity in the pulmonary parenchyma in a varying degree, predominant peripheral, bilateral, lesions' distribution in the posterior, lower, basal regions).

In the process of writing a study radiology report, the attention was paid to the presence of polysegmented sections of the isointense signal corresponding to GGO. Images were also evaluated for the presence of areas of homogeneous hyperintense signal corresponding to pulmonary consolidation on CT scans, as well as for 'crazy-paving' sign, which reflects a combination of GGO and pronounced thickening of interlobular septa interstitium.

2.5. Statistical analysis

Statistical analysis was performed to compare the proportion of patients with lesions in the left and right lungs, as well as in the upper and lower lung lobes of the lungs using the symmetry and homogeneity test for MxN tables with paired samples. A proportion of patients with the presence of lesions on T2WI and on DWI was compared according to the

Table 3
Comparison of the proportion of patients with a different number of lesions in the left and right lung.

Right/left lung	No	1–2 lesions	3 and more lesions	Summary
No	6 (40,0%)	1 (6,7%)	0 (0,0%)	7 (46,7%)
1–2 lesions	2 (13,3%)	1 (6,7%)	0 (0,0%)	3 (20,0%)
3 and more lesions	0 (0,0%)	2 (13,3%)	3 (20,0%)	5 (33,3%)
Summary	8 (53,3%)	4 (26,7%)	3 (20,0%)	15 (100,0%)
P (Symmetry)	0,625			
P (Homogeneity)	0,311			

McNemar criteria. The significance level for all criteria is set to $p < 0.05$.

3. Results

The most distinct changes were visualized on T2WI FSE and DWI. On T2WI changes were identified in 9 (60,0%) patients, on DWI – in 5 (33,3%) patients. In 5 (33,3%) patients lesions of the parenchyma were visualized on T2WI and DWI simultaneously. At the same time, 4 (26.7%) patients had changes in lung tissue only on T2WI. (P(McNemar) = 0,125; OR = 0,00 (95%); kappa = 0,500) (Table 2).

Pulmonary lesions had the following distribution in the lungs: in 8 (53,3%) cases, changes were detected in the right lung, in 7 (46,7%) – in the left lung. Comparison of the proportion of patients with a different

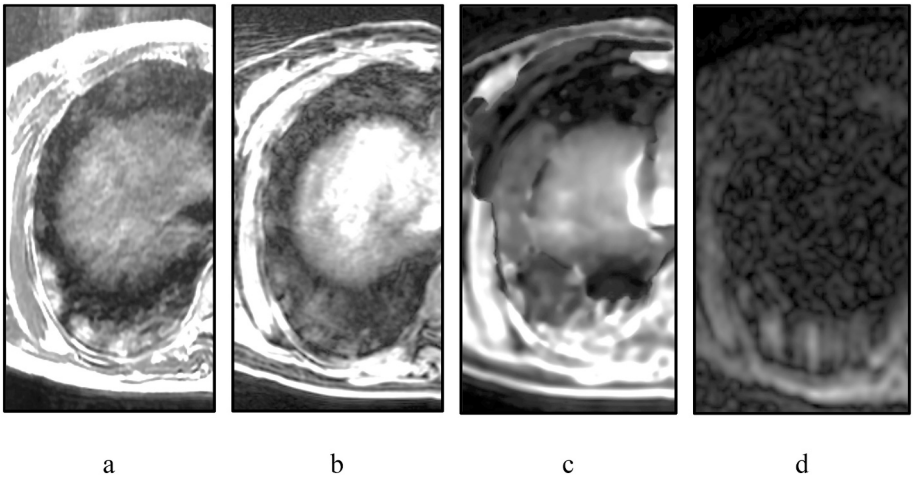

Fig. 1. Chest MRI of 45-year-old woman: a – T2 FSE, b – Lava Flex Water, c – IDEAL Water, d – DWI b = 500 s/mm^2.

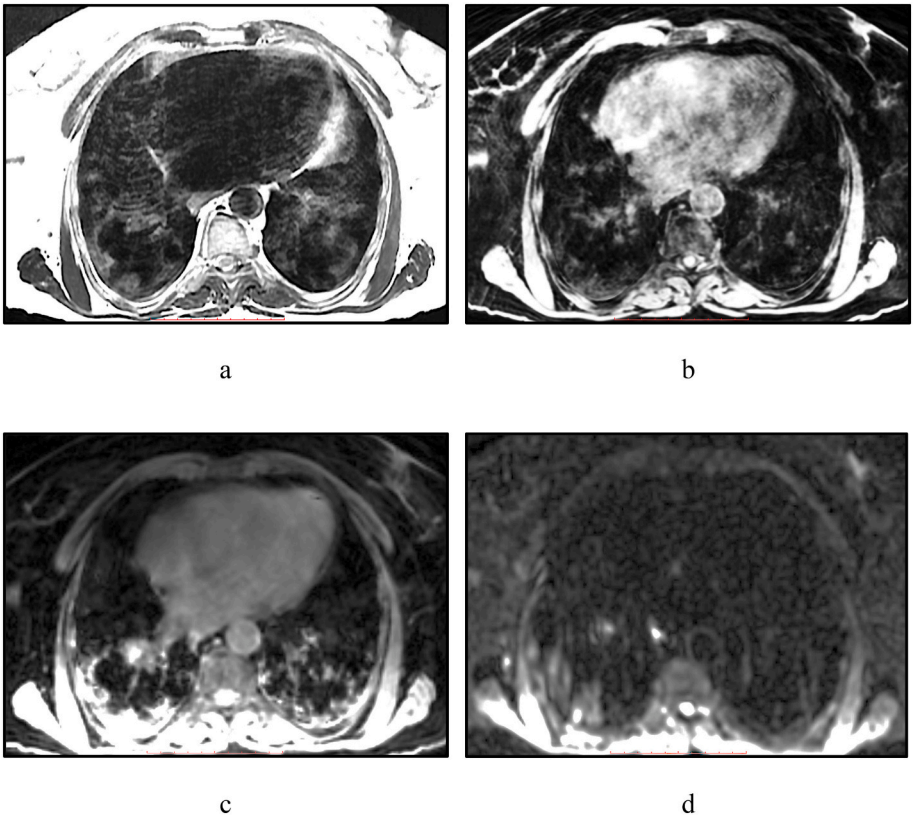

Fig. 2. Chest MRI of 69-year-old woman: a – T2 FSE, b – Lava Flex Water, c – IDEAL Water, d – DWI b = 500 s/mm^2.

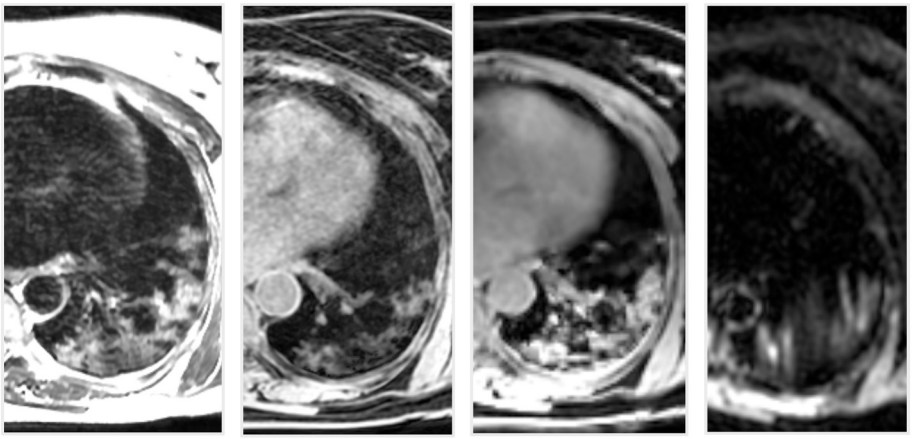

Fig. 3. Chest MRI of 52-year-old woman: a – T2 FSE, b – Lava Flex Water, c – IDEAL Water, d – DWI b = 500 s/mm^2.

number of lesions in the left and right lungs: p = 0,625 and p = 0,31 (Table 3).

Comparison of the proportion of patients with lesions detected on T2 WI and DWI images showed no significant difference ($p = 0.125$). The test for symmetry and uniformity also showed no statistically significant difference in the number of lesions in the left and right lungs ($p = 0.625$ and $p = 0.311$, respectively). Similar results were obtained when comparing the distribution of lesions between upper and lower lobes of lungs ($p = 0.438$ and $p = 0.405$, respectively). Since T2WI is a highly sensitive sequence for detecting fluid in the lung parenchyma, we were able to tell whether there was any lung infiltration. The current study was limited by a small sample size and absence of chest CT scans of all patients.

Examples of MRI cases are presented below.

Case 1: 45-year-old woman. Negative PCR (PCR-).

In basal segments of the lower lobe of the right lung, a section of the inhomogeneously enhanced intensity of the MR signal on T2WI (Fig. 1, a) is identified on the background of the hypointensive lung parenchyma. These changes are less pronounced on Lava Flex Water (Fig. 1, b) and DWI b = 500 s/mm^2 (d), probably due to the lower sensitivity of these pulse sequences to vague pulmonary parenchyma edema. IDEAL Water (Fig. 1, c) represents a significantly amplified signal from this section, however, It is extremely difficult to differentiate it with other signal changes due to the low spatial resolution.

Case 2: 69-year-old woman. Negative PCR (PCR-).

Inhomogeneously enhanced intensity is detected in the basal segments bilaterally on T2WI, which was unclear visualized on Lava Flex Water (Fig. 2, b) on the background of artifacts from chest excursion, while IDEAL Water (Fig. 2, c) shows considerable and extensive changes, which can lead to overdiagnosis of lesions. On DWI b = 500 s/mm^2 (Fig. 2, d), right-sided changes are noted, which might be a predictor of consolidation's development, however, this hypothesis requires confirmation.

Case 3: 52-year-old woman. Positive PCR (PCR+).

On these MRI tomograms a pronounced area of the hyperintense signal is visualized, both on T2WI (Fig. 3, a), and on all other pulse sequences of Lava Flex Water and IDEAL Water (Fig. b, c). This can indicate a lag in visualizing changes in the lungs to Lava Flex Water.

Case 4: 26-year-old woman. Negative PCR (PCR-).

GGOs were detected in S7, 9, 10 (Fig. 4, a) and similar findings were noted in respective segments on all MR-images (Fig. 4, b–f).

Case 5: 26-year-old woman. Negative PCR (PCR-).

GGOs were found in S1, 3 of the right lung (Fig. 5, a) and similar findings were noted in respective segments on all MR-images (Fig. 5, b–f).

4. Discussion

Although most patients with the novel coronavirus disease have mild symptoms and good prognosis, in some cases, it is complicated by severe damage to the respiratory system. CT scan is the most sensitive among all imaging modalities for detection of changes in pulmonary parenchyma [3]. According to the international expert consensus, CT has become the method of choice for patients with suspected viral pneumonia, since its results directly affect patient management [4].

Chest CT in patients with COVID-19 pneumonia most commonly demonstrates bilateral, mainly the right lower lobe distribution of subpleural zones of ground glass opacity with fuzzy edges, air bronchograms. Features of viral pneumonia may be presented even in asymptomatic patients, and lesions may quickly increase or consolidate in 1–3 weeks after onset of symptoms, more often at the second week of the disease. Risk factors for worsening prognosis of the disease are old age, male gender, concomitant chronic conditions [5].

The article presents a comprehensive approach to provide highly informative chest MRI as the alternative, non-ionizing method for patients with COVID-19 under the condition of limited availability of computed tomography. In particular, the higher number of averages allowed to increase probability of obtaining high-quality FSE images. At the same time, the refusal to use non-Cartesian filling of k-space, which is often used in practice, allowed us to avoid blurring along images' periphery. Localization of foci of isointense signal was typical for basal and peripheral pulmonary areas, which corresponds to observed changes at CT scan. Crazy-paving signs on chest MRI and CT scans were visually identical. The main weakness of our research is a small sample, which does not allow us to make confident conclusions, as well as to compare the changes we saw on MRI with a possible CT picture of the same patients. The absolute absence of any criteria that would allow us to link the observed MRI picture to severity of the patient's condition and clinical outcomes complicate the situation.

Magnetic resonance imaging as a method of visualization of the lungs has several disadvantages. Due to the high airiness of the pulmonary tissue, fewer water molecules form a signal, which inevitably reduces the signal-to-noise ratio, resulting in poor-quality images [6]. In addition, susceptibility effects lead to even more pronounced signal attenuation. MRI has low anatomic resolution and is compromised by inevitable artifacts due to breathing movement. However, the ability of MRI to visualize changes in lung structure are constantly expanding due to technical improvement of MRI scanners as well as to appearance of more complex pulse sequences and image post processing [7]. Also, MRI with high magnetic field demonstrated a higher signal to noise ratio during lung imaging [8].

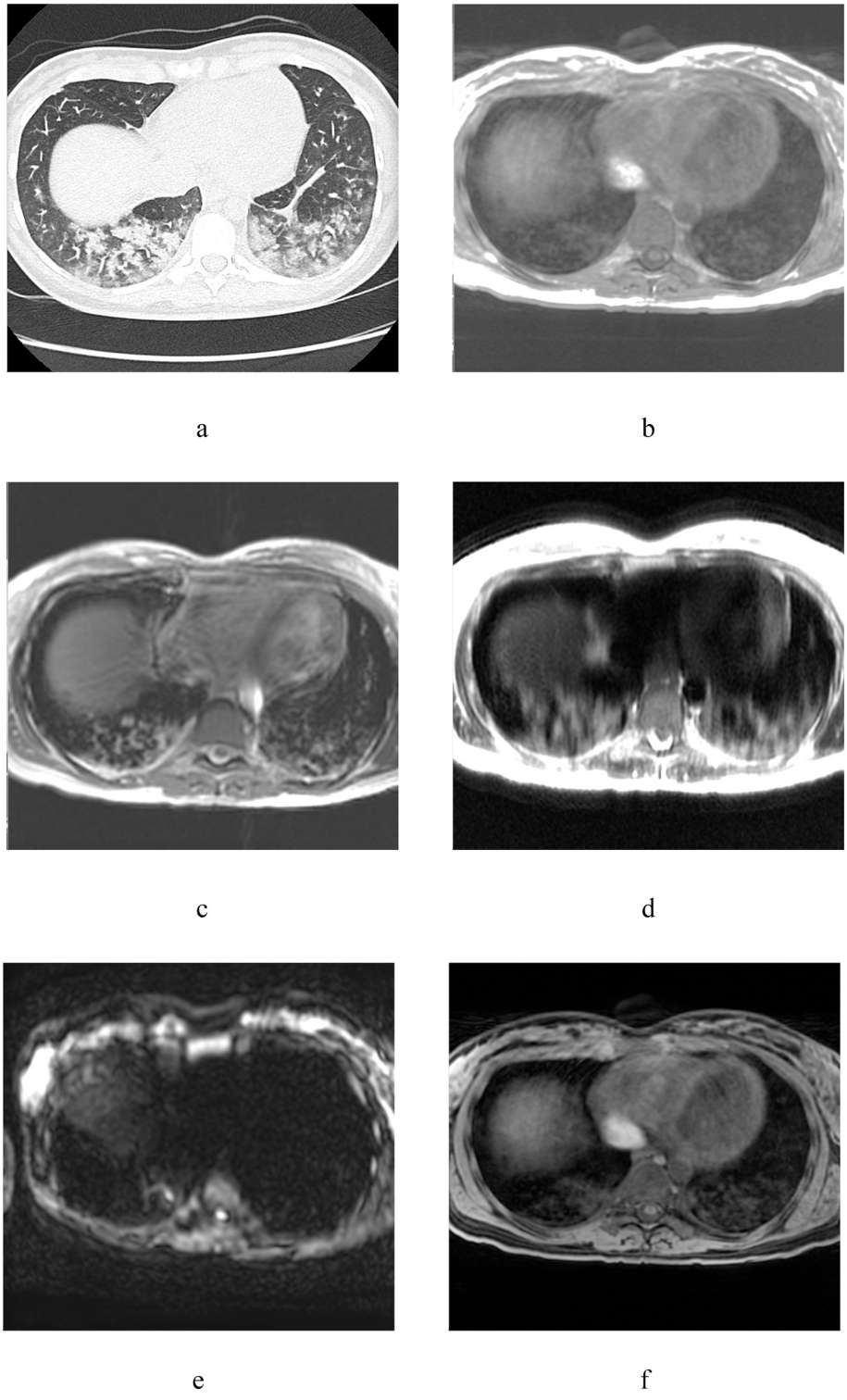

Fig. 4. Chest CT scan and MRI of 26-year-old woman: a – axial CT, b – T1WI in-phase, c – T2 fiesta-WI SE, d – T2WI SSFSE, e – DWI (b = 1000 s/mm^2), f – T1WI 3D GRE FatSat.

Nevertheless, the main question is to what degree detected findings on MRI scans of COVID-19 patients correlate with the radiological changes detected by CT scan. At the moment there are no official clinical recommendations or studies comparing the picture of pathological changes in the lungs obtained with CT and MRI at least in small samples of patients with SARS-CoV-2 pneumonia.

In literature, we found works describing clinical cases, where the authors compared CT and MRI [10–16]. Eibel et al. in their study also compared capabilities of high-resolution MRI and CT to detect pulmonary abnormalities suggesting pneumonia in patients with neutropenia. CT and MRI revealed GGOs in 14 and 16 patients, respectively; in one patient, CT scan performed 3 days later showed GGO at the location previously visualized on MRI, indicating sufficient MRI sensitivity to detect GGO [9]. Consolidation due to infectious pneumonia represented by alveoli filled with fluid, gives a high signal intensity on T2WI. MRI can also differentiate the consolidation associated with fibrous tissues by

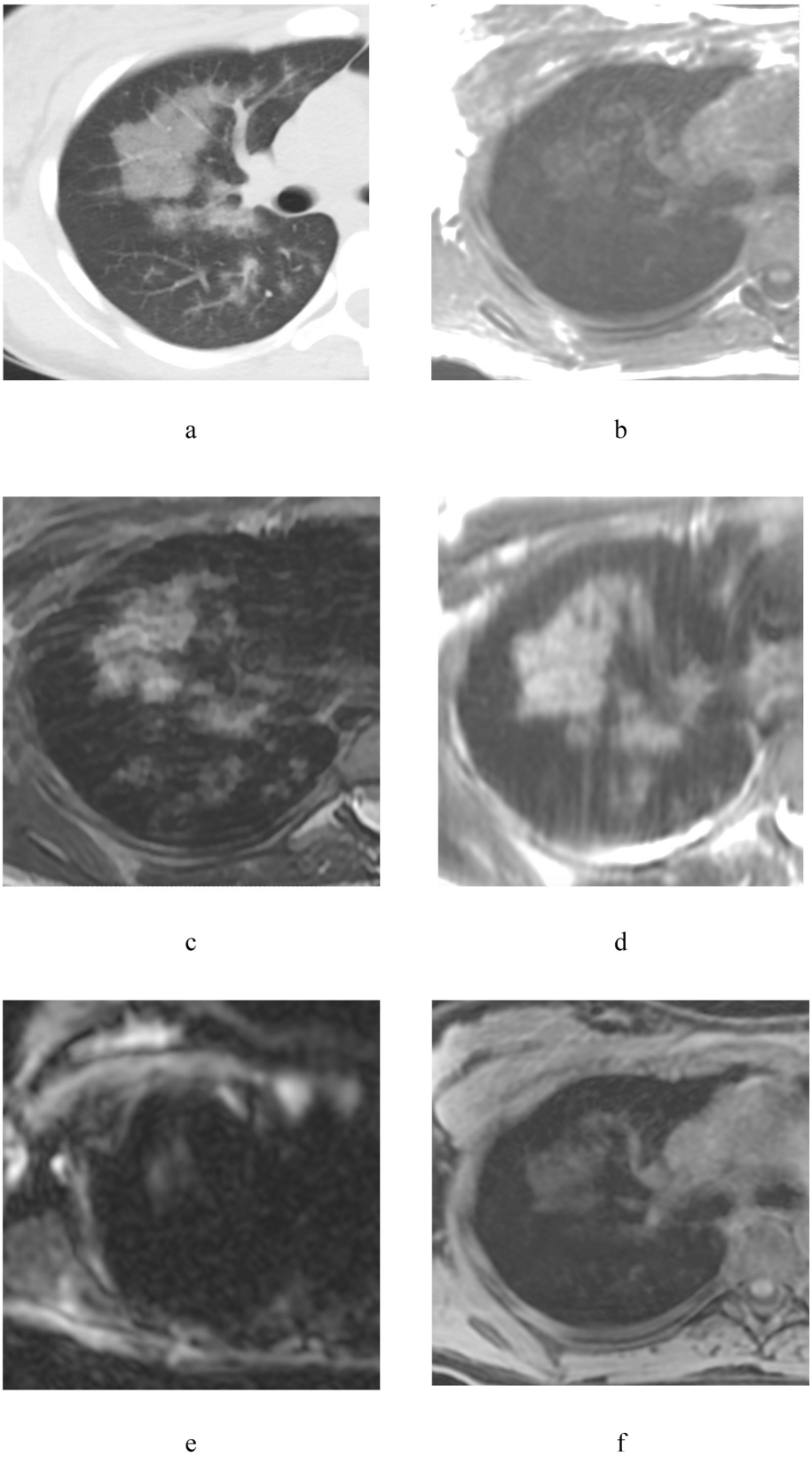

Fig. 5. Chest CT and MRI of 26-year-old woman: a – axial CT, b – T1WI in-phase, c – T2 fiesta-WI SE, d – T2WI SSFSE, e – DWI (b = 1000 s/mm^2), f – T1WI 3D GRE FatSat.

the relatively “short” T2 component. It can be easily distinguished from a focal consolidation associated with pulmonary infarction, which is caused by interalveolar blood. In this case, increase in signal intensity on T1WI will be observed due to the formation of methemoglobin during subacute hemorrhage [10]. A. Ekinci et al. came to the similar conclusions: all MRI sequences were almost perfectly consistent with detected on CT scans areas of consolidations and local increase in lung density. They believe that MRI can be used, particularly in cases where dynamic monitoring of patients is required in order to avoid ionizing radiation exposure [11].

5. Conclusion

The results showed that in case of CT is not available, it is advisable to conduct a chest MRI for patients with suspected or confirmed COVID-19. It is important that in contrast to planar imaging methods, MRI allows us to assess the extent of the lesion and monitor the disease dynamics. It should be noted that the formations on MRI do not look like GGO, therefore in this work we call them “cloudy sky sign”. These data also may be useful in interpreting other studies, such as thoracic spine MRI, cardiac MRI, detecting signs of viral pneumonia in asymptomatic individuals.

Funding

This study was prepared by research (No. in the EGISU: AAAA-A21-121012290079-2) under the Program of the Moscow Healthcare Department "Scientific Support of the Capital’s Healthcare" for 2020-2022.

Ethics approval

The study was approved by Local Ethics Committee of Morozov Children Municipal University Hospital of the Moscow Healthcare Department.

References

[1] Fang Yicheng, Zhang Huangqi, Xie Jicheng, Lin Minjie, Ying Lingjun, Peipei Pang WJ. Sensitivity of Chest CT for COVID-19: Comparison to RT-PCR. Radiology 2020:296. https://doi.org/10.1148/radiol.2020200432.
[2] Long C, Xu H, Shen Q, Zhang X, Fan B, Wang C, et al. Diagnosis of the coronavirus disease (COVID-19): rRT-PCR or CT? Eur J Radiol 2020;126:108961. https://doi.org/10.1016/j.ejrad.2020.108961.
[3] Ai T, Yang Z, Hou H, Zhan C, Chen C, Lv W, et al. Correlation of chest CT and RT-PCR testing for coronavirus disease 2019 (COVID-19) in China: a report of 1014 cases. Radiology 2020;296:E32–40. https://doi.org/10.1148/radiol.2020200642.
[4] Ye Z, Zhang Y, Wang Y, Huang Z, Song B. Chest CT manifestations of new coronavirus disease 2019 (COVID-19): a pictorial review. Eur Radiol 2020;30: 4381–9. https://doi.org/10.1007/s00330-020-06801-0.
[5] Li M. CT features and their role in COVID-19. Radiol Infect Dis 2020:1–4. https://doi.org/10.1016/j.jrid.2020.04.001.
[6] Darçot E, Delacoste J, Dunet V, Dournes G, Rotzinger D, Bernasconi M, et al. Lung MRI assessment with high-frequency noninvasive ventilation at 3 T. Magn Reson Imaging 2020;74:64–73. https://doi.org/10.1016/j.mri.2020.09.006.
[7] Chassagnon G, Martin C, Ben Hassen W, Freche G, Bennani S. High-resolution lung MRI with Ultrashort-TE: 1, 5 or 3 Tesla? Magn Reson Imaging 2019;61:97–103. https://doi.org/10.1016/j.mri.2019.04.015.
[8] Carinci F, Meyer C, Breuer FA, Jakob PM. In vivo imaging of the spectral line broadening of the human lung in a single breathhold. J Magn Reson Imaging 2016; 44:745–57. https://doi.org/10.1002/jmri.25192.
[9] Eibel R, Herzog P, Rieger CT, Reiser MF, Schoenberg SO. Pulmonary abnormalities in Immunocompromised patients : comparative detection with parallel section helical CT. Radiology 2006;241:880–91.
[10] Barreto MM, Rafful PP, Rodrigues RS, Zanetti G, Hochhegger B, Souza AS, et al. Correlation between computed tomographic and magnetic resonance imaging findings of parenchymal lung diseases. Eur J Radiol 2013;82:e492–501. https://doi.org/10.1016/J.EJRAD.2013.04.037.
[11] Ekinci A, Uçarkuş TY, Okur A, Öztürk M, Doğan S. MRI of pneumonia in immunocompromised patients: comparison with CT. Diagn Interv Radiol 2017;23: 22–8. https://doi.org/10.5152/dir.2016.16055.

Vasilev Yuriy Aleksandrovich, Ph. D. Med., Senior Researcher of Technical Monitoring and QA Development, Research and Practical Clinical Center for Diagnostics and Telemedicine Technologies of the Moscow Health Care Department, Moscow, Russia; Imed Clinic, Grozny, Chechen Republic, Russia. Address: 24, st. Petrovka, Moscow, 127051, Russia.

Sergunova Kristina Anatol’evna, Ph. D., Head of Technical Monitoring and QA Development Department, State Budget-Funded Health Care Institution of the City of Moscow «Research and Practical Clinical Center for Diagnostics and Telemedicine Technologies of Moscow Health Care Department». Address: 24, st. Petrovka, Moscow, 127051, Russia.

Alexander Bazhin, Research and Practical Clinical Center for Diagnostics and Telemedicine Technologies of the Moscow Health Care Department, Moscow, Russia; Imed Clinic, Grozny, Chechen Republic, Russia. Address: 24, ul. Petrovka, Moscow, 127051, Russia.

Amir Masri, Imed Clinic, Grozny, Chechen Republic, Russia. Address: 25a, st. Lorsanova, Grozny, 364024, Russia.

Yulia Vasileva, Imed Clinic, Grozny, Chechen Republic, Russia; A.I. Evdokimov Moscow State University of Medicine and Dentistry, Moscow, Russia. Address: 25a, st. Lorsanova, Grozny, 364024, Russia

Semenov Dmitry Sergeevich, Scientist Researcher of Technical Monitoring and QA Development Department, State Budget-Funded Health Care Institution of the City of Moscow «Research and Practical Clinical Center for Diagnostics and Telemedicine Technologies of Moscow Health Care Department». Address: 24, ul. Petrovka, Moscow, 127051, Russia.

Nikita Kudryavtsev, Junior Scientist Researcher of Technical Monitoring and QA Development Department, State Budget-Funded Health Care Institution of the City of Moscow «Research and Practical Clinical Center for Diagnostics and Telemedicine Technologies of Moscow Health Care Department». Address: 24, ul. Petrovka, Moscow, 127051, Russia.

Olga Panina, Junior Scientist Researcher of Technical Monitoring and QA Development Department, State Budget-Funded Health Care Institution of the City of Moscow «Research and Practical Clinical Center for Diagnostics and Telemedicine Technologies of Moscow Health Care Department». Address: 24, ul. Petrovka, Moscow, 127051, Russia.

Anna Khoruzhaya, Junior Scientist Researcher of Technical Monitoring and QA Development Department, State Budget-Funded Health Care Institution of the City of Moscow «Research and Practical Clinical Center for Diagnostics and Telemedicine Technologies of Moscow Health Care Department». Address: 24, ul. Petrovka, Moscow, 127051, Russia.

V.V. Zinchenko, Research and Practical Clinical Center for Diagnostics and Telemedicine Technologies of the Moscow Health Care Department, Moscow, Russia. Address: 24, ul. Petrovka, Moscow, 127051, Russia.

Ahmad Ekaterina Sergeevna, Scientist Researcher of Technical Monitoring and QA Development, State Budget-Funded Health Care Institution of the City of Moscow «Research and Practical Clinical Center for Diagnostics and Telemedicine Technologies of Moscow Health Care Department». Address: 24, ul. Petrovka, Moscow, 127051, Russia.

Petraikin Alexey Vladimirovich, Ph. D. Med., Associate Professor, Senior Researcher of Technical Monitoring and QA Development, State Budget-Funded Health Care Institution of the City of Moscow «Research and Practical Clinical Center for Diagnostics and Telemedicine Technologies of Moscow Health Care Department». Address: 24, ul. Petrovka, Moscow, 127051, Russia.

Vladzymyrskyy Anton Vjacheslavovich, M. D. Med., Deputy Director for Science, State Budget-Funded Health Care Institution of the City of Moscow «Research and Practical Clinical Center for Diagnostics and Telemedicine Technologies of Moscow Health Care Department». Address: 24, ul. Petrovka, Moscow, 127051, Russia.

Aslanbek Validovich Midaev, Imed Clinic, Grozny, Chechen Republic, Russia.

Morozov Sergey Pavlovich, M. D. Med., Professor, Director, State Budget-Funded Health Care Institution of the City of Moscow «Research and Practical Clinical Center for Diagnostics and Telemedicine Technologies of Moscow Health Care Department».